Critical Reviews in Biochemistry and Molecular Biology

http://informahealthcare.com/bmg
ISSN: 1040-9238 (print), 1549-7798 (electronic)
Editor: Michael M. Cox
Crit Rev Biochem Mol Biol, 2014; 49(5): 400–412
 DOI: 10.3109/10409238.2014.925421

informa
healthcare

REVIEW ARTICLE

Dynamics of the ClpP serine protease: A model for self-compartmentalized proteases

Kaiyin Liu, Adedeji Ologbenla, and Walid A. Houry

Department of Biochemistry, University of Toronto, Toronto, Ontario, Canada

Abstract

ClpP is a highly conserved serine protease present in most bacterial species and in the mitochondria of mammalian cells. It forms a cylindrical tetradecameric complex arranged into two stacked heptamers. The two heptameric rings of ClpP enclose a roughly spherical proteolytic chamber of about 51 Å in diameter with 14 Ser–His–Asp proteolytic active sites. ClpP typically forms complexes with unfoldase chaperones of the AAA+ superfamily. Chaperones dock on one or both ends of the ClpP double ring cylindrical structure. Dynamics in the ClpP structure is critical for its function. Polypeptides targeted for degradation by ClpP are initially recognized by the AAA+ chaperones. Polypeptides are unfolded by the chaperones and then translocated through the ClpP axial pores, present on both ends of the ClpP cylinder, into the ClpP catalytic chamber. The axial pores of ClpP are gated by dynamic axial loops that restrict or allow substrate entry. As a processive protease, ClpP degrades substrates to generate peptides of about 7–8 residues. Based on structural, biochemical and theoretical studies, the exit of these polypeptides from the proteolytic chamber is proposed to be mediated by the dynamics of the ClpP oligomer. The ClpP cylinder has been found to exist in at least three conformations, extended, compact and compressed, that seem to represent different states of ClpP during its proteolytic functional cycle. In this review, we discuss the link between ClpP dynamics and its activity. We propose that such dynamics also exist in other cylindrical proteases such as HslV and the proteasome.

Keywords

Catalysis, ClpP, degaradation, dynamics, protease

History

Received 16 April 2014
Revised 12 May 2014
Accepted 14 May 2014
Published online 10 June 2014

Introduction

Proteins are one of the most complex macromolecules in the cell. They are responsible for carrying out the majority of cellular activities thus making protein homeostasis, or proteostasis, a tightly regulated process. Protein folding is mediated by the activities of molecular chaperones such as members of the Heat Shock Protein (Hsp) family, which usually couple ATP hydrolysis with iterative cycles of substrate binding and release to help proteins achieve their native state. On the other hand, protein degradation in the cell is mediated by self-compartmentalized, energy-dependent proteases (De Mot *et al*., 1999; Pickart & Cohen, 2004). These proteases include the well-studied serine protease Caseinolytic protease P (ClpP), the threonine protease Heat shock locus V (HslV, also known as ClpQ) (Chuang *et al*., 1993) and the 20S Core Particle (CP) of the proteasome present in eukaryotes, archaea, and some bacteria (Humbard & Maupin-Furlow, 2013; Inobe & Matouschek, 2014). All the proteases share the common feature of having their proteolytic active sites buried within the cylindrical-like structure formed by the oligomerization of the protease subunits and, thus, they are named self-compartmentalized proteases or chambered proteases (Pickart & Cohen, 2004).

Self-compartmentalized proteases typically have limited proteolytic activity against well-folded protein substrates that cannot enter their proteolytic chamber, however, they can degrade such folded proteins with the help of AAA+ (ATPases Associated with diverse cellular Activities) chaperone components. These chaperones form the cap for the chambered protease and use ATP binding and hydrolysis to aid with protein unfolding and translocation into the proteolytic chamber of the protease. In *Escherichia coli*, the partner chaperones for ClpP are ClpA or ClpX. For HslV, the partner chaperone is HslU. For the proteasome, the CP is capped by the Regulatory Particle (RP), which is composed of at least 19 subunits in eukaryotes, 9 subunits form the ''base'' complex and around 10 subunits form the ''lid'' of the cap (Tomko & Hochstrasser, 2013). Six of the subunits of the ''base'' complex are AAA+ proteins.

ClpP was first purified and studied in *E. coli* (Katayama-Fujimura *et al*., 1987; Katayama *et al*., 1988). *Escherichia coli* ClpP (EcClpP) consists of 207 amino acids and is expressed as a proenzyme (Figure 1; Maurizi *et al*., 1990).

Address for correspondence: W. A. Houry, 1 King's College Circle, Medical Sciences Building, Department of Biochemistry, University of Toronto, Toronto, Ontario M5S 1A8, Canada. Tel: 416 946-7141. Fax: 416 978-8548. E-mail: walid.houry@utoronto.ca

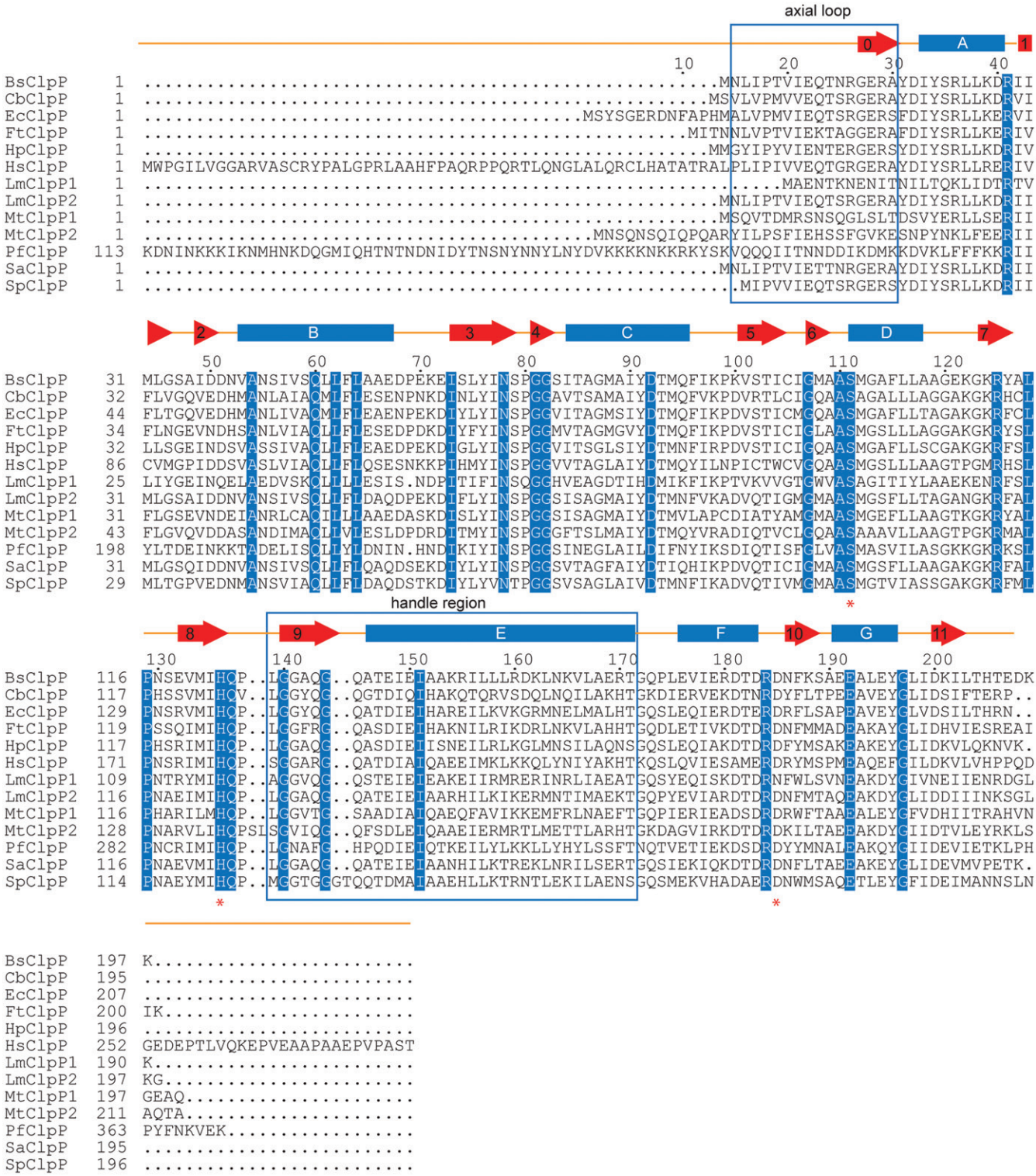

Figure 1. Sequence alignment of ClpPs for which X-ray structures are available. Residues shaded in blue are 100% conserved across all the listed ClpPs. Asterisks indicate the catalytic triad residues Ser, His and Asp. Secondary structure and residue numbering refer to EcClpP sequence. Structural alignment was done using STRAP (Gille & Frommel, 2001). Boxes refer to α helices, while arrows refer to β strands. Note that LmClpP1 has a natural substitution of Asn for the Asp residue in the catalytic triad. Also, note that PfClpP has an extended N-terminus and that the sequence beginning at residue 113 is shown. The PfClpP X-ray structure was solved for an N-terminally truncated protein having instead residues corresponding to a His_6-tag and tobacco etch virus cut site at the N-terminus. All the other ClpP sequences shown are of the full-length wild-type protein. Throughout the manuscript, residue numbering follows that of UniProtKB database (UniProt, 2014). The UniprotKB identifiers for the sequences shown are as follows: BsClpP is P80244 (CLPP_BACSU), CbClpP is B6J0W0 (CLPP_COXB2), EcClpP is P0A6G7 (CLPP_ECOLI), FtClpP is Q5NH47 (CLPP_FRATT), HpClpP is P56156 (CLPP_HELPY), HsClpP is Q16740 (CLPP_HUMAN), LmClpP1 is E1UFC3 (E1UFC3_LISML), LmClpP2 is E1UAZ0 (E1UAZ0_LISML), MtClpP1 is P9WPC5 (CLPP1_MYCTU), MtClpP2 is P9WPC3 (CLPP2_MYCTU), PfClpP is O97252 (O97252_PLAF7), SaClpP is P63786 (CLPP_STAAW), and SpClpP is P63788 (CLPP_STRR6). See colour version of this figure at www.informahealthcare.com/bmg.

The proenzyme undergoes autoproteolysis removing the N-terminal 14 amino acids to create the mature ClpP sequence of 193 amino acids (Maurizi *et al*., 1990). *E. coli* ClpP forms tetradecamers of two identical stacked homoheptamers (Figure 2A–C) (Gersch *et al*., 2012). All 14 subunits of the *E. coli* ClpP tetradecamer have protease activity. If the organism has multiple copies of the *clpP* gene, for example as in *Listeria monocytogenes* where there are two

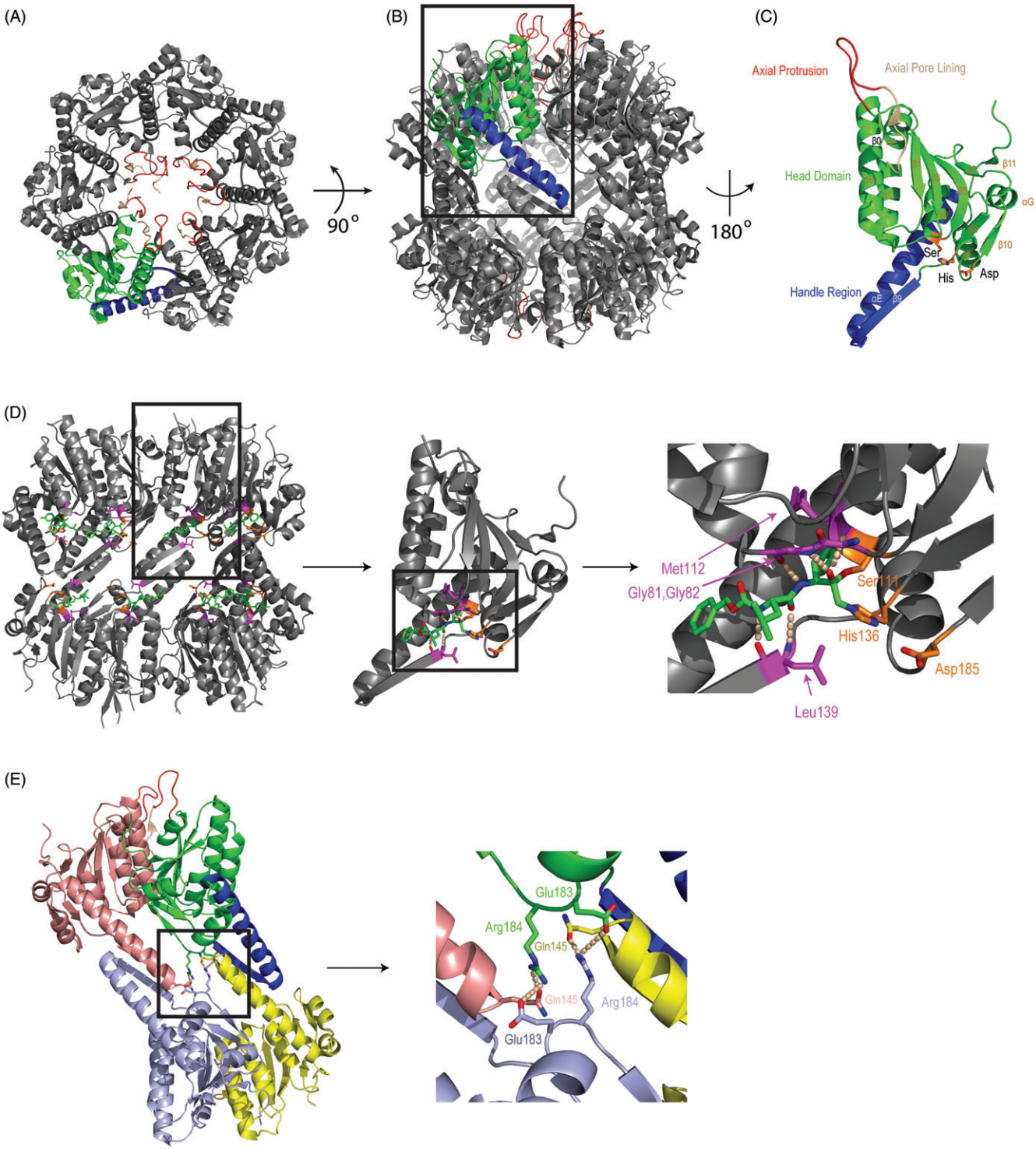

Figure 2. Overview of ClpP structure. (A–C) Extended EcClpP crystal structure is displayed as the canonical ClpP protease structure (PDB 1YG6). The axial pore lining of the axial loop is colored in wheat, the axial protrusion part of the axial loop is colored in red, the head domain is colored in green and the handle domain is colored in blue. (A) Top view and (B) side view of EcClpP tetradecamer with one monomer colored. (C) EcClpP monomer magnified from box in panel B. Secondary structure elements are labeled. The catalytic triad residues are colored orange. (D) Cross section of the EcClpP tetradecamer with a substrate Z-LY-CMK (in green) covalently bound at the active site (PDB 3FZS). The active site residues are colored in orange. Residues of β4 and β9 involved in coordinating the substrate (Gly81, Gly82, Met112 and Leu139) are colored in purple. Hydrogen bonds are indicated by wheat dots. (E) The arginine sensor of EcClpP (PDB 1YG6). Four monomers of the ClpP tetradecamer are shown. Two hydrogen bonding networks involving Arg184, Glu183, and Gln145 are indicated by wheat dots. All figures were drawn using PyMOL (DeLano, 2002). See colour version of this figure at www.informahealthcare.com/bmg.

ClpP isoforms (Figure 1), it is proposed that the enzyme may form heterotetradecamers (Zeiler *et al*., 2013). In EcClpP, the catalytic triad is formed by the residues Ser111, His136 and Asp185 (Figures 1 and 2C).

Although HslV is also considered as a Clp family member, it has a different oligomerization scheme than ClpP. HslV protomer is approximately 19 kDa. HslV was found to arrange into dodecamers to form a complex of approximately 230 kDa consisting of two identical homohexamers (Bochtler *et al*., 1997; Kessel *et al*., 1996). All 12 subunits of the dodecamer have protease activity. HslV has sequence similarity with the β subunits of the eukaryotic and archaebacterial proteasomes (Bochtler *et al*., 1997). Interestingly, *E. coli* HslV active site threonine residue is residue number two in the sequence after methionine residue number one. The other residues of the EcHslV active site are Lys33 and Ser125 (Bochtler *et al*., 1997).

The oligomerization architecture of the 20S CP of the proteasome is much more complex. The proteasome is found in eukaryotes, archaebacteria, and the Gram-positive actinobacteria. Similar to HslV, the proteasome is also a threonine protease. In general, the CP consists of two heptamers formed from β proteasome subunits sandwiched between two heptamers formed from α proteasome subunits. In archaea, such as *Thermoplasma acidophilum*, and actinobacteria, such as *Mycobacterium tuberculosis*, all the α and β proteasome subunits are identical, and it is expected that all of the β subunits have protease activity. In eukaryotes, there are seven distinct α and seven distinct β subunits and not all β subunits are active (Humbard & Maupin-Furlow, 2013).

The high-resolution X-ray crystal structure of ClpP has been solved from various different organisms (Table 1). In some of these organisms, ClpP structures in different conformations have been observed. This directly points to the dynamic nature of ClpP. Here, we discuss the link between the structural dynamics of self-compartmentalized proteases, specifically that of ClpP and the proteasome, and their proteolytic activity. Residue numbers used in this review refer to the sequences in Figure 1 of the unprocessed proteases as obtained from the UniprotKB database (UniProt, 2014).

Table 1. Summary of solved X-ray structures of ClpP.

Organism	Protein	Conformation
Bacillus subtilis	WT (3KTG)[a]	Extended
	WT (3TT6)[b]	Compressed
Coxiella burnetii	WT (3Q7H)[c]	Extended
Escherichia coli	WT (1YTF)[d]	Extended
	WT (1YG6)[e]	Extended
	V20A (1YG8)[e]	Extended
	WT (2FZS)[f]	Extended
	A153C (3HLN)[g]	Compact
Francisella tularensis	WT (3P2L)[h]	Extended
Helicobacter pylori	WT (2ZL0)[i]	Extended
	S99A (2ZL3)[i]	Extended
Homo sapiens (mitochondrial)	WT (1TG6)[j]	Extended
Listeria monocytogenes	WT ClpP1 (4JCQ)[k]	Compact
	N165D ClpP1 (4JCR)[k]	Extended
	WT ClpP2 (4JCT)[k]	Extended
Mycobacterium tuberculosis	WT ClpP1 (2CE3)[l]	Compact
Plasmodium falciparum	WT (2F6I)[m]	Compact
Staphylococcus aureus	WT (3QWD)[n],	Extended
	(3V5E)[o], (3STA)[p]	Extended
	S98A (3V5I)[o]	Extended
	E137A (4EMP)[q]	Extended
	WT (4EMM)[q]	Compact
	WT (3ST9)[p]	Compressed
Streptococcus pneumoniae	A140P (1Y7O)[r]	Compact

PDB file codes are given in parenthesis.
[a]Lee *et al*. (2010); [b]Lee *et al*. (2011); [c]Deposited in PDB but not published in a manuscript; [d]Wang *et al*. (1997); [e]Bewley *et al*. (2006); [f]Szyk & Maurizi (2006); [g]Kimber *et al*. (2010); [h]Deposited in PDB but not published in a manuscript; [i]Kim & Kim (2008); [j]Kang *et al*. (2004); [k]Zeiler *et al*. (2013); [l]Ingvarsson *et al*. (2007); [m]El Bakkouri *et al*. (2010); [n]Geiger *et al*. (2011); [o]Gersch *et al*. (2012); [p]Zhang *et al*. (2011); [q]Ye *et al*. (2013); [r]Gribun *et al*. (2005).

General overview of ClpP structure

The X-ray crystal structure of ClpP displays an N-terminal axial loop region (Figure 2A). This region is proposed to function in restricting the size of the ClpP axial substrate entry pores present on both ends of the ClpP cylinder (Bewley *et al*., 2006; Gribun *et al*., 2005; Zhang *et al*., 2011), as well as, in mediating the interaction between the ClpP protease and its cognate AAA+ ATPase (Figure 2A–C; Bewley *et al*., 2006; Gribun *et al*., 2005; Jennings *et al*., 2008a; Kim *et al*., 2001). Protein substrates destined to be degraded by the ClpP protease must enter the catalytic chamber through the narrow axial pores lined by these N-terminal axial loops (Figure 2A and B).

The N-terminal axial loop can be divided into two parts. The first part, termed ''axial pore lining'', comprises hydrophobic residues Ala15–Ile21 in EcClpP (Figures 1 and 2C in wheat). These residues are stabilized by interactions with the head domain (see below) and line the axial pore (Bewley *et al*., 2006; Gribun *et al*., 2005). The second part of the N-terminal axial loop, termed ''axial protrusion'', which comprises residues Glu22–Ser30 in EcClpP (Figures 1 and 2C in red), contains predominantly charged or hydrophilic residues and form an extended loop protruding from the axial pore (Bewley *et al*., 2006; Gribun *et al*., 2005). The exact interactions involving this region of ClpP is currently unclear as this loop was found in many different conformations in ClpPs from different organisms.

Following the N-terminal axial loop is the head domain, which forms the bulk of the ClpP protease chamber (Figures 1 and 2A–C in green). The head domain contains the catalytic triad residues: Ser111, His136 and Asp185. Through crystallographic analysis, it was determined that the protein substrate to be degraded is held close to the active site via interactions with the head domain, specifically: β4, β9 and H-bonding network with the wall of the ClpP chamber (Figure 2D; Szyk & Maurizi, 2006). These interactions involve residues Gly81, Gly82, Met112 and Leu139 in addition to Ser111 (Figure 2D). The structure of the head domain was found to be largely invariable across the various ClpPs from the different organisms (Figure 3).

The handle domain of ClpP, which consists of β strand 9 and helix E is a strand-turn-helix motif and forms the

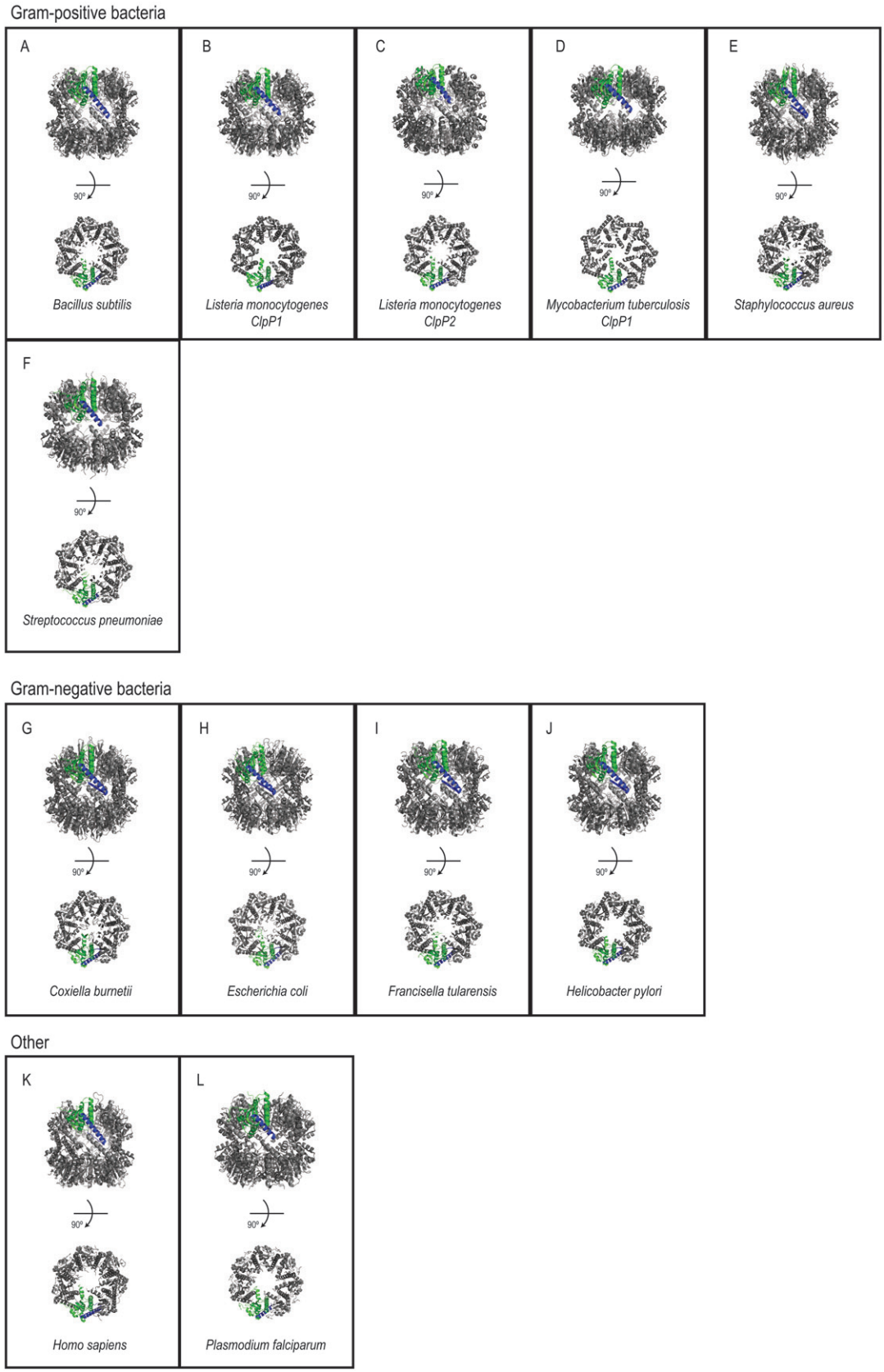

Figure 3. Structures of ClpP from different organisms. Side and top views of ClpP tetradecameric structures from Gram-positive (A–F) and Gram-negative (G–J) bacteria and from other organisms (K,L). All the structures are of WT ClpP except for SpClpP. For a complete list of all of the crystallized ClpP structures in various conformational states, refer to Table 1. The structures shown are as follows: (A) ClpP from *B. subtilis* in the extended state (PDB 3KTG); (B) ClpP1 from *L. monocytogenes* in the compact state (PDB 4JCQ); (C) ClpP2 from *L. monocytogenes* in the compact state (PDB 4JCT); (D) ClpP1 from *M. tuberculosis* in the compact state (PDB 2CE3); (E) ClpP from *S. aureus* in the extended state (PDB 3STA); (F) ClpP from *S. pneumoniae* A140P in the compact state (PDB 1Y7O); (G) ClpP from *C. burnetii* in the extended state (PDB 3Q7H); (H) ClpP from *E. coli* in the extended state (PDB 3TT6); (I) ClpP from *F. tularensis* in the extended state (PDB 3P2L); (J) ClpP from *H. pylori* in the extended state (PDB 2ZL0); (K) Mitochondrial ClpP from *H. sapiens* in the extended state (PDB 1TG6); (L) ClpP from *P. falciparum* in the compact state (PDB 2F6I). See colour version of this figure at www.informahealthcare.com/bmg.

equatorial wall of the protease chamber (Gribun *et al*., 2005; Zhang *et al*., 2011; Figures 1 and 2A–C in blue). Originally, it was proposed that this domain mediates the formation of the ClpP tetradecameric double-ring structure from the single-ring heptamers. The handle domains from opposing monomers of the heptameric rings were found to interdigitate with each other in the solved X-ray crystal structures of tetradecameric ClpP (Wang *et al*., 1998). However, as discussed below, it has subsequently been shown that the handle domain is quite elastic (Gribun *et al*., 2005; Sprangers *et al*., 2005) and, instead, important residues in the head domain are proposed to mediate inter-ring contacts of ClpP. In *Staphylococcus aureus* ClpP (SaClpP), for example, R171 (R184 in EcClpP) of the head domain in one heptameric ring is involved in H-bonding and charged–charged interactions with residues D170 (E183 in EcClpP) and Q132 (Q145 in EcClpP) of the corresponding protomer in the opposing heptameric ring (Figure 2E; Zhang *et al*., 2011). Mutation of R171 in SaClpP to alanine or lysine resulted in the formation of heptamers (Gersch *et al*., 2012). This finding has also been corroborated for *Streptococcus pneumoniae* ClpP (SpClpP). SpClpP with R171G (corresponds to R171 in SaClpP) or E170A (corresponds to D170 in SaClpP) mutations formed heptamers and mixtures of heptamers and tetradecamers, respectively (Gribun *et al*., 2005). As such, R171 in SpClpP or SaClpP, or the equivalent R184 in EcClpP, is referred to as the sensor of the ClpP oligomeric state (Gersch *et al*., 2012).

The proteolytic chamber of EcClpP is a sphere of about 50 Å in diameter and can accommodate several hundred residues of unstructured substrate (Wang *et al*., 1997). Due to the high local concentration of the 14 active sites, simple proximity drives the binding of substrates to the active sites and enhances the efficient hydrolysis of polypeptides that enter the chamber (Baker & Sauer, 2012). In addition, the 14 active sites are close to each other in space, separated by about 25 Å between two neighboring active site Ser residues within one heptameric ring (Figure 2D). Hence, a polypeptide can bind to multiple active sites simultaneously, thus, increasing avidity and tandem cleavage events. Indeed, ClpP is considered to be a processive protease whose proteolytic activity generates peptides with an average size distribution of about 7–8 residues with no accumulation of intermediates (Jennings *et al*., 2008b).

The structures of WT and/or mutant ClpPs from *Bacillus subtilis* (BsClpP), *Coxiella burnetii* (CbClpP), *Escherichia coli* (EcClpP), *Francisella tularensis* (FtClpP), *Helicobacter pylori* (HpClpP), *Homo sapiens* mitochondria (HsClpP), *Listeria monocytogenes* (LmClpP), *Mycobacterium tuberculosis* (MtClpP), *Plasmodium falciparum* (PfClpP), *Staphylococcus aureus* (SaClpP) and *Streptococcus pneumoniae* (SpClpP) have been successfully crystallized (El Bakkouri *et al*., 2010; Gribun *et al*., 2005; Ingvarsson *et al*., 2007; Kang *et al*., 2004; Kim & Kim, 2008; Lee *et al*., 2010; Wang *et al*., 1997; Zeiler *et al*., 2013; Zhang *et al*., 2011; Figure 3). Their primary sequences share high sequence similarity (Figure 1). All these ClpPs have the Ser, His, Asp catalytic residues, except for LmClpP1, which has an Asn instead of the Asp (Figure 1).

Dynamic axial loops of ClpP: ClpP N-terminus forms a loop that regulates entry of substrates into the chamber

Since the catalytic sites in ClpP are accessible only via the two axial pores on each end of the ClpP cylinder (Figures 2A and B and 4A), the N-terminal axial loops adopt an open or a closed conformation to allow or restrict, respectively, the translocation of polypeptides into the catalytic chamber. The axial loops are also important for mediating the interaction of ClpP with the cognate ATPase (Bewley *et al*., 2006; Gribun *et al*., 2005; Martin *et al*., 2007). Mutating or deleting residues in the loop region abrogates the ClpP-cognate ATPase interaction.

The N-terminal sequence of mature ClpP is highly conserved across several species (Gribun *et al*., 2005; Kang *et al*., 2004; Figure 1). The axial loops are very flexible based on the diverse structural studies in which the loops were either partially or totally untraceable. Crystal structures that successfully mapped the N-terminal loops have shown the loops to adopt either an ''up'' or ''down'' conformation (Figure 4A). In the up conformation, the loops extend out of the apical surface of the cylinder. A β-hairpin structure formed by the residues at the N-terminus has been observed in *E. coli*, *S. pnuemoniae*, and human ClpP (Gribun *et al*., 2005; Kang *et al*., 2004; Szyk & Maurizi, 2006). In the down conformation, the loops are tucked within the proteolytic chamber (Bewley *et al*., 2006; Szyk & Maurizi, 2006).

Evidence points to the ClpP axial loops acting as a gate and regulating the rate of peptide entry into the ClpP proteolytic chamber. ClpP mutants with truncated axial loops degraded model peptide substrates at a much faster rate than wild-type ClpP (Gribun *et al*., 2005). Using cryoelectron microscopy, it has been shown that the ClpP axial loops switch from closed to open conformation upon ClpA binding to ClpP resulting in the opening of the entrance axial pores (Effantin *et al*., 2010a,b).

The open and closed states of ClpP are linked to the up and down conformations of the axial loops (Bewley *et al*., 2006; Effantin *et al*., 2010b). From the structure of *E. coli* ClpP by Bewley et al. (2006), six of the seven N-terminal loops from one heptameric ring protruded about 10–15 Å beyond the ClpP apical surface; this was termed the up conformation (Bewley *et al*., 2006; Effantin *et al*., 2010b). The seventh loop did not protrude out of the chamber and was similar to the structure of the seven N-terminal loops from the second heptameric ring, termed the down conformation (Bewley *et al*., 2006; Effantin *et al*., 2010b; Figure 4A). The up conformation was initially thought to represent a closed state of ClpP. This was because the seventh N-terminal loop that does not protrude outside the apical surface seemed to lie across the surface of the channel of ClpP. On the other hand, the down conformation, with all the seven loops incompletely visualized and non-protruding, was assumed to be in an open conformation (Figure 4A). Cryo-EM reconstruction of ClpP has, however, shown that the reverse is the case and that the channel is open when the loops are up (Effantin *et al*., 2010b). Hence, controversy exists as to which conformation of the axial loops facilitates better substrate entry into the ClpP proteolytic chamber.

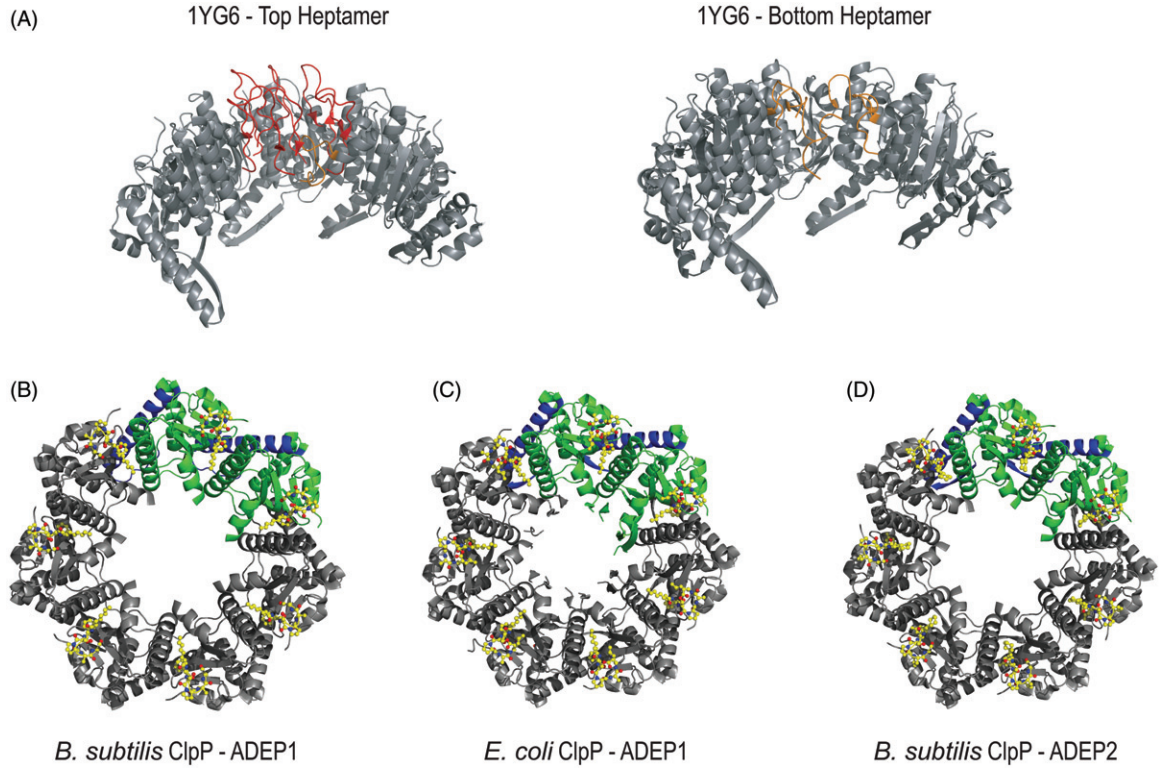

Figure 4. Different conformations of the ClpP axial loops. (A) N-terminal loops of *E. coli* ClpP (PDB 1YG6) in both the up and down conformations. The loops colored in red are in the up conformation and extend out of the axial pore. The loop colored in orange is in the down conformation and remains within the ClpP cylinder. (B–D) Co-crystal structure of ClpP from *B. subtilis* with ADEP1 (PDB 3KTI) (B), of ClpP from *E. coli* with ADEP1 (PDB 3MT6) (C) and of ClpP from *B. subtilis* with ADEP2 (PDB 3KTK) (D). The ADEP molecules are colored in yellow and represented as sticks. See colour version of this figure at www.informahealthcare.com/bmg.

In the open conformation, formation of a β-hairpin by the N-terminus was shown to be vital for efficient translocation of polypeptides into the degradation chamber (Alexopoulos *et al*., 2013; Gribun *et al*., 2005). Mutation of Ile21 to Pro in EcClpP, which prevents the formation of the β-hairpin by introducing a kink, decreased the hydrolysis rate of EcClpP to 9% (Alexopoulos *et al*., 2013). The β-hairpin in EcClpP is stabilized by a hydrophobic groove formed by residues 33 and 46 of the same protomer and 35, 38, 60 and 63 of the neighboring protomer in the head domain of EcClpP. The groove serves as an anchor point for the hydrophobic residues 16–21 at the N-terminus of the axial loop (Alexopoulos *et al*., 2013; Gribun *et al*., 2005).

A study conducted via synchrotron hydroxyl radical footprinting coupled with kinetic experiments, suggested a model for proteolysis by EcClpAP in which the axial loops play a vital role in promoting catalysis (Jennings *et al*., 2008a). In this model, the ATP-bound form of ClpA interacts with ClpP, thus, causing the ClpP axial loops to assume the ''up'' conformation. This widens the ClpP axial pore and provides the substrate with easy access to the ClpP proteolytic chamber. The switching of the axial loops to the ''down'' conformation then stimulates the hydrolysis of the acyl-enzyme intermediate at the active site through a yet undetermined mechanism, but which probably involves allosteric effects (Jennings *et al*., 2008a).

Acyldepsipeptides (ADEPs) are a class of antibiotics that have been shown to bind ClpP and to cause it to degrade proteins in the absence of ClpX or ClpA (Brotz-Oesterhelt *et al*., 2005). ADEPs can cause unregulated proteolysis *in vivo* thus leading to cell death particularly in Gram-positive bacteria. Crystal structures of *E. coli* and *B. subtilis* ClpP have been solved in complex with ADEPs (Figure 4B–D; Lee *et al*., 2010; Li *et al*., 2010). ADEPs have been found to bind the same hydrophobic pockets on the ClpP apical surface where the IGF/IGL loops of the cognate ATPases bind. It is thus assumed that ADEPs are a model for the interaction between ClpP and its cognate ATPases. As a result, the ADEP-ClpP cocrystal structures have provided new insights into the gating mechanism of ClpP, although the interpretation of the structures has also been controversial as to whether the ADEPs loosen or rigidify the β-hairpin conformation of the axial loops (Alexopoulos *et al*., 2013). Nevertheless, ADEPs seem to cause the ClpP N-terminus to adopt a conformation in which the axial pore is widened to about 20 Å in diameter, thus, opening the gate for polypeptides to enter the degradation chamber. Based on mutational studies conducted on the N-terminus of both *E. coli* and *B. subtilis* ClpP, it was suggested that the mechanisms that stabilize the open conformation of the axial gate are conserved in both Gram-positive and Gram-negative bacteria (Alexopoulos *et al*., 2013).

More recently, high-throughput screening led to the discovery of new classes of compounds that activate ClpP in the absence of ClpX or ClpA. These novel compounds possessed structures that were significantly different from ADEPs and were termed Activators of Self-Compartmentalizing Proteases (ACPs; Leung *et al*., 2011).

Five different compounds from four different structural classes were successfully identified as ACPs by the screen. These compounds all activated ClpP in the absence of its cognate ATPases, and the compounds were found to bind to the same hydrophobic pockets on ClpP as the ADEPs. Obtaining the ACP–ClpP co-crystal structure should shed further insights into the ClpP gating mechanism.

Dynamic handle region of ClpP: elasticity of the E helix

The handle domain of ClpP, β strand 9 and helix E (Figures 1 and 2A–C), has been shown to be a very dynamic region of the protein and to adopt different conformations (Gersch *et al*., 2012; Sprangers *et al*., 2005; Ye *et al*., 2013; Zeiler *et al*., 2013; Zhang *et al*., 2011). The handle domain is proposed to be involved in regulating peptide release from the ClpP protease (Gribun *et al*., 2005; Kimber *et al*., 2010; Sprangers *et al*., 2005). The conformational state of the handle domain has also been found to correlate with the activity of the ClpP protease (Gersch *et al*., 2012; Zeiler *et al*., 2013).

Information on the elasticity of the handle region was initially based on studies of SpClpP and EcClpP (Gribun *et al*., 2005; Kimber *et al*., 2010; Sprangers *et al*., 2005). It was found that truncation of helix E or insertion of prolines in that helix did not affect the formation of ClpP tetradecameric double-ring structure. However, when the X-ray crystal structure of SpClpP with mutation of A140 in helix E to Pro was solved, no electron density was found for residues 123–138 in the handle region (Figure 5A and B). These residues were proposed to reside inside the protease lumen (Gribun *et al*., 2005). In addition, the active site residues of the SpClpP(A140P) mutant were found to be distorted leading to an inactive enzyme. Importantly, the structure revealed the formation of equatorial side pores measuring about 5 Å × 10 Å (Figure 5B). These pores were lined by hydrophobic residues: Arg147, His166 and Glu170 of one monomer; Ile138, Ala139 and Glu141 of a second monomer from the same ring; and Arg171, Asp172, Asn173 and Trp174 of a third monomer from the opposite ring (Gribun *et al*., 2005). When compared to the reported structure of WT EcClpP, SpClpP(A140P) structure was more compact as the heptamers moved closer together by about 6 Å resulting in a smaller catalytic chamber (Figure 5A and B).

Subsequently, the dynamics of the handle regions of EcClpP were studied using NMR Transverse Relaxation Optimized Spectroscopy (TROSY) of methyl groups (Sprangers *et al*., 2005). This technique allows the study of structural dynamics in large protein complexes. These NMR experiments are typically based on the specific labeling of methyl groups in Leu, Ile, and Val. Methyl groups are useful spectroscopic probes of protein structure and dynamics and their resonances are intense and well dispersed. In this study, it was clearly established that the handle domain is highly dynamic and can adopt at least two distinct conformational states. Biochemically, an EcClpP(A153C) mutant displayed increased retention of model peptides under oxidizing conditions because of the formation of disulfide bonds between the E helices of two opposing subunits in each of the heptameric rings. The same mutant ClpP under reducing conditions did not trap any products (Sprangers *et al*., 2005). This indicated that the handle region may need to be flexible to allow for proper product release. Furthermore, under oxidizing conditions, EcClpP(A153C) did not have protease activity, while under reducing conditions this mutant enzyme was active albeit at 32 times lower activity compared to WT, however, the K_M of this mutant remained the same as WT (Kimber *et al*., 2010). These studies strongly suggested that the flexibility of the handle region is required for ClpP activity.

The X-ray crystal structure of oxidized EcClpP(A153C) was then solved (Kimber *et al*., 2010). The handle region was found to be disordered in the structure resulting in the formation of equatorial side pores (Figure 5C). In addition, oxidized EcClpP(A153C) was in a compact state compared to that of WT EcClpP (Figure 5C versus 5A). The two heptameric rings in the structure were shifted closer to each other due to the surfaces of opposing αE helices sliding over one another.

In silico analysis of the extended EcClpP structure using normal mode analysis revealed that the structure of the compact EcClpP(A153C) mutant represents a probable structure of EcClpP undergoing thermal motion (Kimber *et al*., 2010). Furthermore, careful analysis of the many ClpP structures deposited in the Protein Data Bank determined that, while some ClpPs were crystallized in an extended state, others have been crystallized trapped in different compacted states (Figure 3; Kimber *et al*., 2010).

The structures observed, the biochemical data obtained, and theoretical considerations led us to propose that ClpP naturally samples these different states in a dynamic manner caused by the elasticity in the handle region (Kimber *et al*., 2010). The cycling through these different states might be regulated by bound cognate ATPases and is likely required for ClpP to degrade proteins entering its catalytic chamber through the axial pores and for releasing generated peptides via transiently formed equatorial side pores (Figure 5D), thus allowing the protease to act processively.

Dynamic handle region of ClpP: Three conformational states of the ClpP cylinder

Currently, three states for ClpP have been observed by X-ray crystallography: extended, compact and compressed based on the height of the ClpP cylinder and the structure of the handle region (Table 1). The extended state has been seen for ClpP from *C. burnetii* (Deposited in PDB but not published in a manuscript), *E. coli* (Wang *et al*., 1997), *F. tularensis* (Deposited in PDB but not published in a manuscript), *H. pylori* (Kim & Kim, 2008), *L. monocytogenes* ClpP2 (Zeiler *et al*., 2013) and human mitochondria (Kang *et al*., 2004). The compact state has been observed for ClpP from *E. coli* (Kimber *et al*., 2010), *S. pneumoniae* (Gribun *et al*., 2005), *M. tuberculosis* (Ingvarsson *et al*., 2007), *L. monocytogenes* ClpP1 (Zeiler *et al*., 2013), *P. falciparum* (El Bakkouri *et al*., 2010; Vedadi *et al*., 2007), *B. subtilis* (Lee *et al*., 2011) and *S. aureus* (Geiger *et al*., 2011; Zhang *et al*., 2011). The more compacted state, termed

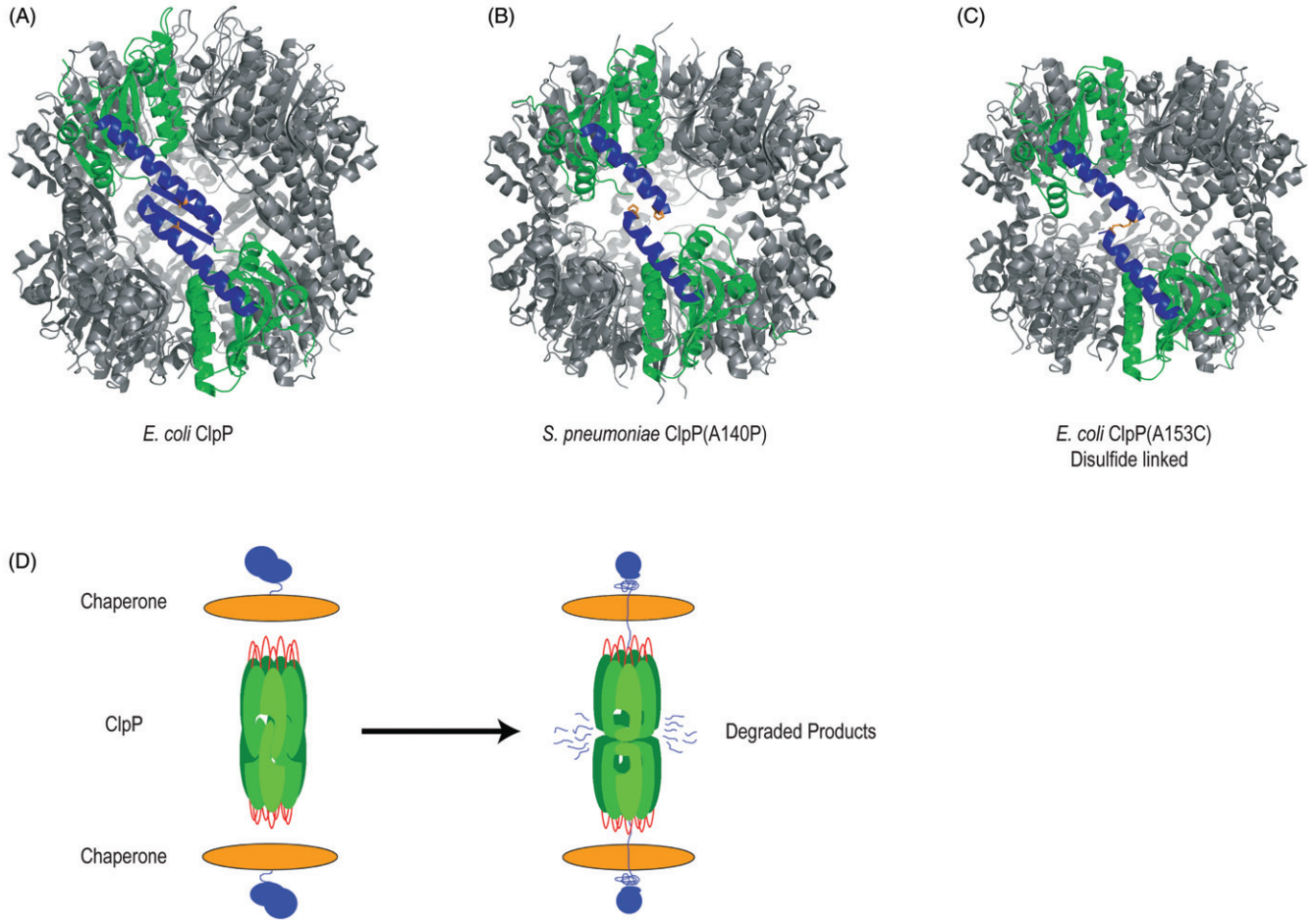

Figure 5. Different conformations of the ClpP cylinder and its implications on ClpP catalytic activity. (A) Structure of WT EcClpP (PDB 1YG6) with two opposing monomers of the heptamers colored. The handle domain is colored blue, is well ordered and β9 is clearly seen. A153 is in orange sticks. (B) Structure of SpClpP(A140P) mutant (PDB 1Y7O) with two opposing monomers of the heptamers colored. The proline residue is in orange; the handle domain is in blue; β9 is not structured. (C) Structure of EcClpP(A153C) mutant (PDB 3HLN) in the oxidized state with two opposing monomers of the heptamers colored. The cysteine residue is in orange; the handle domain is in blue; β9 is not structured. (D) Proposed degradation mechanism and peptide product release by ClpP. See colour version of this figure at www.informahealthcare.com/bmg.

compressed state, has been observed for ClpP from *B. subtilis* (Lee *et al*., 2011) and *S. aureus* (Geiger *et al*., 2011; Ye *et al*., 2013; Zeiler *et al*., 2013; Zhang *et al*., 2011).

High resolution X-ray structures have been solved for SaClpP in all three states (Gersch *et al*., 2012; Zhang *et al*., 2011; Figure 6). In the extended conformation, the handle region of each ClpP monomer is well ordered in the double heptameric structure (Figure 6A,D). Residues Arg171 and Asp170 help to stabilize the tetradecamer and, through an H-bonding network with residue Gln132, help keep the handle domain in an extended ''straight'' conformation (Figure 6J). H-bonding of Arg171 with Asp170 on the opposing heptamer causes a conformational change to the active site residue Asp172, leading to the correct orientation of the SaClpP catalytic triad (Figure 6G; Gersch *et al*., 2012; Zeiler *et al*., 2013). In addition, Gln132 is proposed to form H-bonding interaction with Glu135, which further stabilizes the handle domain in an extended conformation (Gersch *et al*., 2012). Gly127, Gly128 and Gly131 were also found to be important in mediating the formation of extended SaClpP tetradecamers, as residues from subunits in opposing rings were found to form an anti-parallel β-sheet upon tetradecamerization, which leads to the active site His123 attaining an activate conformation, i.e. in bridging the active site residues Asp172 and Ser98 (Gersch *et al*., 2012). Mutation of all three glycine residues to alanine resulted in the formation of inactive heptamers (Gersch *et al*., 2012). In the extended state, the surface of the ClpP equatorial region is continuous and unbroken (Zhang *et al*., 2011).

In the compact state, the E helix in the handle region is partly unstructured and β9 is completely disordered (Zhang *et al*., 2011; Figure 6B,E). The Arg171–Asp170–Gln132 H-bonding network is not formed (Figure 6K). In addition, the Ser–His–Asp catalytic triad is not properly oriented and likely corresponds to an inactive state of ClpP (Figure 6H).

The structure of the compressed state is drastically different from both the extended and compacted structures. The structure of compressed SaClpP was solved by two different groups in 2011 (Zhang *et al*., 2011; Geiger *et al*., 2011). Both groups found that the compressed SaClpP was inactive and that the cylinder was shorter by about 10 Å along the axial direction (Figure 6C). In this state, there are 14 equatorial side pores formed at the ring–ring interface that are up to 6 Å in diameter, depending on the conformations of the side chains. The β9 strand is disordered and the E helix is broken at residue Lys145, forming an 80° kink and resulting

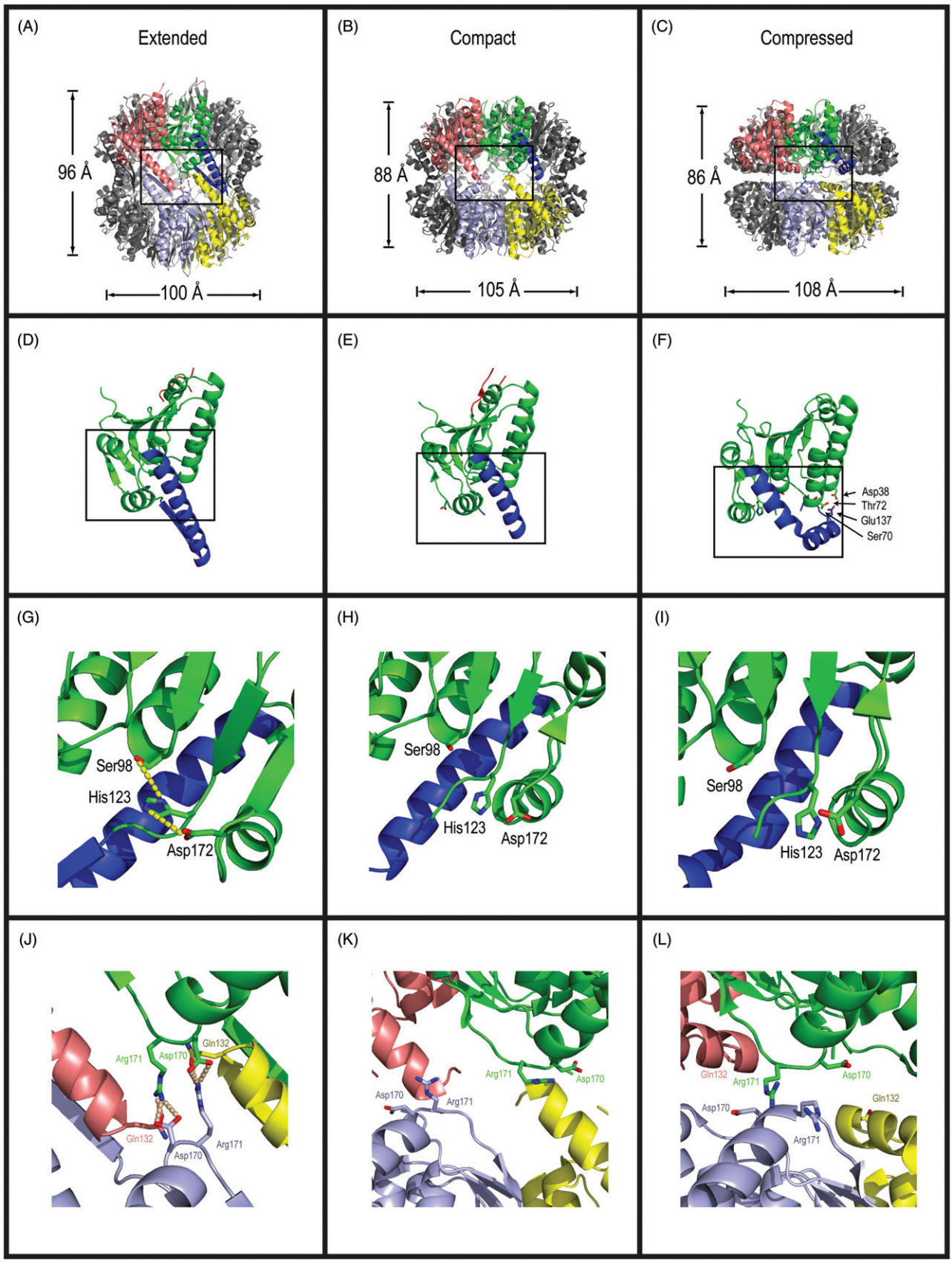

Figure 6. Three conformational states of SaClpP. (A–C) The extended (PDB 3STA), compact (PDB 4EMM) and compressed (PDB 3ST9) structures of SaClpP tetradecamer are shown in A, B and C, respectively. Four protomers are colored. One protomer is colored in green (head domain) and blue (handle region). The other three protomers are colored as indicated. (D–F) Magnification of the green and blue monomer in panels A–C. In F, the residues proposed to be involved in stabilizing the compressed state are labeled. (G–I) Magnification of the boxed region as seen from inside the proteolytic chamber of panels D–F. The active site residues are labeled. Hydrogen bonds are indicated by wheat dots. (J–L) Magnification of the boxed region in panels A–C showing the orientation of the Arg171, Asp170 and Gln132 residues. Hydrogen bonds are indicated by wheat dots. See colour version of this figure at www.informahealthcare.com/bmg.

in the formation of two smaller helices (Figure 6F), which extend into the protease chamber. The kinked E helix causes the two heptameric rings to further approach each other (Figure 6C). This state of the helix is stabilized by H-bonding interactions between Glu137 residue located at the tip of helix E with residues Asp38, Ser70 and Thr72 in the head domain (Ye *et al*., 2013; Zhang *et al*., 2011; Figure 6F). Interestingly, SaClpP(E137A) mutant has no peptidolytic activity, indicating that this residue is important in the substrate proteolysis cycle, which probably requires the kinked state of the E helix (Ye *et al*., 2013). It should be noted, however, that the compressed state of BsClpP showed no density corresponding to helix E or β9 strand (Lee *et al*., 2011). In the compressed state, all of the H-bonding and charged–charged interactions stabilizing the tetradecamer, including the Arg171–Asp170–Gln132 interaction network, are not formed (Zhang *et al*., 2011; Figure 6L). This suggests that a significantly weakened tetradecameric structure in the compressed state (Zhang *et al*., 2011). Furthermore, the catalytic triad is not properly oriented (Figure 6I).

Molecular dynamics (MD) simulations on the solved structures of the extended and compressed SaClpP structures revealed that the ''dynamic region'' in the handle domain of ClpP between residues His123 and Lys145 is highly flexible. Using the extended SaClpP heptamer structure as a starting point, this segment of helix E was found to move from extended to the kinked conformation (Ye *et al*., 2013; Zhang *et al*., 2011). Interestingly, the His123 residue, which is part of the catalytic triad, was observed to shift away from its active conformation in the extended SaClpP structure to an inactive conformation in the compressed SaClpP structure. Thus, MD simulations suggest that the compressed SaClpP structure is proteolytically inactive as observed by crystallography (Figure 6I). Moreover, the simulations revealed that the compact conformation of SaClpP represents a stable intermediate in the transition from extended to compressed SaClpP (Ye *et al*., 2013). Based on the simulations, the N-terminal part of helix E was observed to undergo an unfolding/refolding process, moving from the single continuous helix E in extended SaClpP to the partially disordered helix E from residue H123 to A140 in compact SaClpP. This is then followed by partial refolding leading to the kinked helix E at residue Lys145 in compressed SaClpP (Ye *et al*., 2013).

The role of ClpP dynamics in product release

There are two different proposed mechanisms by which peptides generated upon substrate cleavage by ClpP are released from the proteolytic chamber. The first mechanism proposes that the axial pores function in both substrate entry and peptide product release. This proposal is problematic because this mode of substrate release would imply that the AAA+ chaperone, which can bind simultaneously to both ends of the ClpP cylinder, has to periodically dissociate from ClpP to allow for product release, thus, interrupting the processive degradation by the enzyme and, as a result, should generate incompletely degraded products. Such incomplete degradation products are not observed. Furthermore, it has been shown that dissociation of EcClpA from EcClpP has a $t_{1/2}$ of 22 min, which is longer than the $t_{1/2}$ for the degradation of many substrates, thus, the ClpAP complex seems to be stable for multiple cycles of substrate degradation (Jennings *et al*., 2008a; Singh *et al*., 1999). Also, electron microscopy studies of ClpAP and ClpXP complexes showed that hybrid complexes can also form where the two ATPases cap the opposite ends of ClpP at the same time (Ortega *et al*., 2004). Taken together, we argue that it is unlikely that the axial pores function in both substrate entry and product release.

The second mechanism for product release, which was put forward by our group (Gribun *et al*., 2005; Kimber *et al*., 2010; Sprangers *et al*., 2005), proposes that the transiently formed equatorial side pores mediate product release (Figure 5D). Emerging studies described above show the plasticity of the handle domain and the observation of transient side pores seem to support this mode of product release. However, the exact mechanism driving product release still remains enigmatic. It could be possible that accumulation of peptide products within the ClpP chamber would cause all of the ClpP subunits to convert from extended to compact or compressed states in a concerted fashion to facilitate product release. The side pores in this case are estimated to have a diameter of about 6 Å (Gersch *et al*., 2012; Gribun *et al*., 2005). Alternatively, a few of the subunits in ClpP could switch from the extended to the compact or compressed state, generating equatorial side pores for product release (Gersch *et al*., 2012). The pores in this case are reported to be approximately 12 Å in diameter (Gersch *et al*., 2012). While we favor the second mechanism, further experiments are needed to elucidate the exact molecular details causing product release from ClpP.

Dynamics of the proteasome

Proteasome dynamics have been explored using methyl TROSY NMR experiments (Religa *et al*., 2010; Sprangers & Kay, 2007), which are suited to study the dynamics of the proteasome CP complex (about 600 kDa). Methyl TROSY NMR experiments on the archeabacterium *Thermoplasma acidophilum* CP, which consists of two heptameric β rings sandwiched between two heptameric α rings (Figure 7A and B), showed that the β rings had little effect on the structure or dynamics of the α rings. It was determined that the N-terminal 12 residues of the α ring were mobile and form a gate into the proteasome chamber (Sprangers & Kay, 2007).

Subsequently, detailed study of the gating residues of the α subunits revealed that they occupy two distinct states: ''out'' where the gating residues are well outside the proteolytic chamber or ''in'' where the gating residues are well inside the chamber (Figure 7C; Religa *et al*., 2010). Mutations, which lead to a more stable out conformation, had remarkably higher peptidolytic activity as compared to WT (Religa *et al*., 2010). Similar to ClpP, deletion of gating residues 3–11 of the N-terminus produced a mutant with the highest peptidolytic activity (Religa *et al*., 2010). 11S activator cap binding to the CP increased peptidolytic activity in a titratable manner. However, an Y8G/D9G mutant of the α subunit did not show a titratable increase in peptidolytic activity possibly because key interactions between the gating residues and the 11S were abolished in the mutant leading to a closed α pore (Figure 7C; Religa *et al*., 2010).

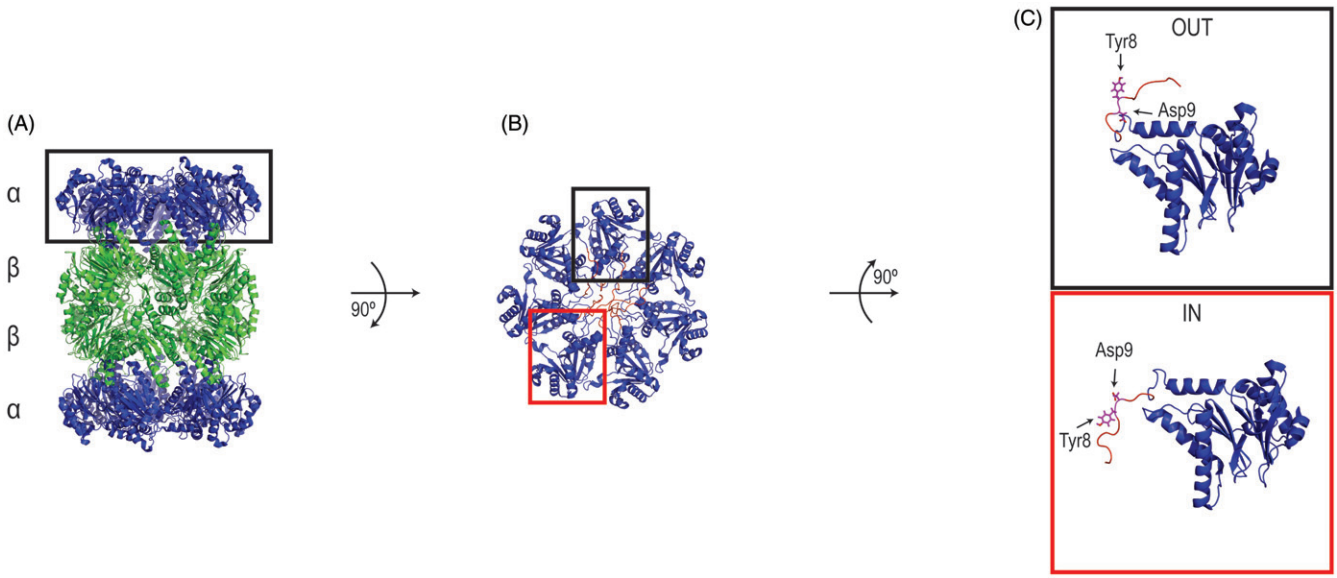

Figure 7. Dynamics of the gating residues in the *T. acidophilum* proteasome. (A) X-ray crystal structure of the 20S proteasome of *T. acidophilum* (PDB 1PMA). (B) Top view of *T. acidophilum* proteasome showing the NMR structure of the α subunits (PDB 2KU1). The dynamic gating residues (1–12) studied by TROSY-NMR are colored in red. Five of the α subunits have their N-terminal residues in the ''out'' conformation and two have those residues in the ''in'' conformation. (C) Top and bottom panels show the magnification of the black-boxed and red-boxed regions in B, respectively. Residues Tyr8 and Asp9, which are proposed to interact with the 11S activator cap, are in purple. See colour version of this figure at www.informahealthcare.com/bmg.

It seems the N-terminus gating residues of the proteasome CP are responsible for similar functions as the axial loop residues of ClpPs. In future experiments, it would be interesting to determine whether residues in the β subunit of the proteasome CP behave similarly as the handle domain of ClpPs.

Concluding remarks

Of all the self-compartmentalized proteases, ClpP has been studied in most detail. Understanding the dynamics and mechanism of action of ClpP is crucial as it could help shed more light into the other cylindrical proteases like the HslV and the proteasome. Here, we have highlighted two main features of the dynamics of these cylindrical proteases. The first feature relates to the use of dynamic axial loops to control entry of substrates into the catalytic chamber. The second feature relates to the dynamics of the body of the cylinder itself that affects the proteolysis activity and the exit of generated peptide products. We propose that such dynamics might also regulate peptide release from HslV and the inner rings consisting of the β subunits of the proteasome. These features seem to represent an inherent property of these enzymes. However, it is very likely that the bound AAA+ chaperones, substrates, and other cofactors can regulate these dynamics to influence the functional proteolytic cycle of these proteases. Further experimental and theoretical studies on these highly conserved proteases will shed more light into such regulation.

Acknowledgements

Kaiyin Liu was the recipient of the Ontario Graduate Scholarship and the Life Sciences Award from the University of Toronto. Adedeji Ologbenla was the recipient of a University of Toronto Fellowship from the Department of Biochemistry.

Declaration of interest

The authors declare no competing interests. This work was supported by a grant from the Canadian Institutes of Health Research (MOP-130374) to WAH.

References

Alexopoulos J, Ahsan B, Homchaudhuri L, *et al*. (2013). Structural determinants stabilizing the axial channel of ClpP for substrate translocation. Mol Microbiol 90:167–80.

Baker TA, Sauer RT. (2012). ClpXP, an ATP-powered unfolding and protein-degradation machine. Biochim Biophys Acta 1823:15–28.

Bewley MC, Graziano V, Griffin K, *et al*. (2006). The asymmetry in the mature amino-terminus of ClpP facilitates a local symmetry match in ClpAP and ClpXP complexes. J Struct Biol 153:113–28.

Bochtler M, Ditzel L, Groll M, *et al*. (1997). Crystal structure of heat shock locus V (HslV) from *Escherichia coli*. Proc Natl Acad Sci USA 94:6070–4.

Brotz-Oesterhelt H, Beyer D, Kroll HP, *et al*. (2005). Dysregulation of bacterial proteolytic machinery by a new class of antibiotics. Nat Med 11:1082–7.

Chuang SE, Burland V, Plunkett III G, *et al*. (1993). Sequence analysis of four new heat-shock genes constituting the hslTS/ibpAB and hslVU operons in *Escherichia coli*. Gene 134:1–6.

De Mot R, Nagy I, Walz J, *et al*. (1999). Proteasomes and other self-compartmentalizing proteases in prokaryotes. Trends Microbiol 7: 88–92.

DeLano WL. (2002). The PyMOL molecular graphics system. Palo Alto (CA): DeLano Scientific.

Effantin G, Ishikawa T, De Donatis GM, *et al*. (2010a). Local and global mobility in the ClpA AAA+ chaperone detected by cryo-electron microscopy: functional connotations. Structure 18:553–62.

Effantin G, Maurizi MR, Steven AC. (2010b). Binding of the ClpA unfoldase opens the axial gate of ClpP peptidase. J Biol Chem 285: 14834–40.

El Bakkouri M, Pow A, Mulichak A, *et al*. (2010). The Clp chaperones and proteases of the human malaria parasite *Plasmodium falciparum*. J Mol Biol 404:456–77.

Geiger SR, Bottcher T, Sieber SA, *et al*. (2011). A conformational switch underlies ClpP protease function. Angew Chem Int Ed Engl 50: 5749–52.

Gersch M, List A, Groll M, *et al*. (2012). Insights into structural network responsible for oligomerization and activity of bacterial virulence regulator caseinolytic protease P (ClpP) protein. J Biol Chem 287: 9484–94.

Gille C, Frommel C. (2001). STRAP: editor for STRuctural Alignments of Proteins. Bioinformatics 17:377–8.

Gribun A, Kimber MS, Ching R, *et al*. (2005). The ClpP double ring tetradecameric protease exhibits plastic ring–ring interactions, and the N termini of its subunits form flexible loops that are essential for ClpXP and ClpAP complex formation. J Biol Chem 280: 16185–96.

Humbard MA, Maupin-Furlow JA. (2013). Prokaryotic proteasomes: nanocompartments of degradation. J Mol Microbiol Biotechnol 23: 321–34.

Ingvarsson H, Mate MJ, Hogbom M, *et al*. (2007). Insights into the inter-ring plasticity of caseinolytic proteases from the X-ray structure of *Mycobacterium tuberculosis* ClpP1. Acta Crystallogr D Biol Crystallogr 63:249–59.

Inobe T, Matouschek A. (2014). Paradigms of protein degradation by the proteasome. Curr Opin Struct Biol 24C:156–64.

Jennings LD, Bohon J, Chance MR, *et al*. (2008a). The ClpP N-terminus coordinates substrate access with protease active site reactivity. Biochemistry (Mosc) 47:11031–40.

Jennings LD, Lun DS, Medard M, *et al*. (2008b). ClpP hydrolyzes a protein substrate processively in the absence of the ClpA ATPase: mechanistic studies of ATP-independent proteolysis. Biochemistry (Mosc) 47:11536–46.

Kang SG, Maurizi MR, Thompson M, *et al*. (2004). Crystallography and mutagenesis point to an essential role for the N-terminus of human mitochondrial ClpP. J Struct Biol 148:338–52.

Katayama-Fujimura Y, Gottesman S, Maurizi MR. (1987). A multiple-component, ATP-dependent protease from *Escherichia coli*. J Biol Chem 262:4477–85.

Katayama Y, Gottesman S, Pumphrey J, *et al*. (1988). The two-component, ATP-dependent Clp protease of *Escherichia coli*. Purification, cloning, and mutational analysis of the ATP-binding component. J Biol Chem 263:15226–36.

Kessel M, Wu W, Gottesman S, *et al*. (1996). Six-fold rotational symmetry of ClpQ, the *E. coli* homolog of the 20S proteasome, and its ATP-dependent activator, ClpY. FEBS Lett 398:274–8.

Kim DY, Kim KK. (2008). The structural basis for the activation and peptide recognition of bacterial ClpP. J Mol Biol 379:760–71.

Kim YI, Levchenko I, Fraczkowska K, *et al*. (2001). Molecular determinants of complex formation between Clp/Hsp100 ATPases and the ClpP peptidase. Nat Struct Biol 8:230–3.

Kimber MS, Yu AY, Borg M, *et al*. (2010). Structural and theoretical studies indicate that the cylindrical protease ClpP samples extended and compact conformations. Structure 18:798–808.

Lee BG, Kim MK, Song HK. (2011). Structural insights into the conformational diversity of ClpP from *Bacillus subtilis*. Mol Cells 32: 589–95.

Lee BG, Park EY, Lee KE, *et al*. (2010). Structures of ClpP in complex with acyldepsipeptide antibiotics reveal its activation mechanism. Nat Struct Mol Biol 17:471–8.

Leung E, Datti A, Cossette M, *et al*. (2011). Activators of cylindrical proteases as antimicrobials: identification and development of small molecule activators of ClpP protease. Chem Biol 18:1167–78.

Li DH, Chung YS, Gloyd M, *et al*. (2010). Acyldepsipeptide antibiotics induce the formation of a structured axial channel in ClpP: a model for the ClpX/ClpA-bound state of ClpP. Chem Biol 17:959–69.

Martin A, Baker TA, Sauer RT. (2007). Distinct static and dynamic interactions control ATPase-peptidase communication in a AAA+ protease. Mol Cell 27:41–52.

Maurizi MR, Clark WP, Katayama Y, *et al*. (1990). Sequence and structure of Clp P, the proteolytic component of the ATP-dependent Clp protease of *Escherichia coli*. J Biol Chem 265:12536–45.

Ortega J, Lee HS, Maurizi MR, *et al*. (2004). ClpA and ClpX ATPases bind simultaneously to opposite ends of ClpP peptidase to form active hybrid complexes. J Struct Biol 146:217–26.

Pickart CM, Cohen RE. (2004). Proteasomes and their kin: proteases in the machine age. Nat Rev Mol Cell Biol 5:177–87.

Religa TL, Sprangers R, Kay LE. (2010). Dynamic regulation of archaeal proteasome gate opening as studied by TROSY NMR. Science 328: 98–102.

Singh SK, Guo F, Maurizi MR. (1999). ClpA and ClpP remain associated during multiple rounds of ATP-dependent protein degradation by ClpAP protease. Biochemistry (Mosc) 38:14906–15.

Sprangers R, Gribun A, Hwang PM, *et al*. (2005). Quantitative NMR spectroscopy of supramolecular complexes: dynamic side pores in ClpP are important for product release. Proc Natl Acad Sci USA 102: 16678–83.

Sprangers R, Kay LE. (2007). Quantitative dynamics and binding studies of the 20S proteasome by NMR. Nature 445:618–22.

Szyk A, Maurizi MR. (2006). Crystal structure at 1.9A of *E. coli* ClpP with a peptide covalently bound at the active site. J Struct Biol 156: 165–74.

Tomko Jr RJ, Hochstrasser M. (2013). Molecular architecture and assembly of the eukaryotic proteasome. Annu Rev Biochem 82: 415–45.

UniProt C. (2014). Activities at the Universal Protein Resource (UniProt). Nucleic Acids Res 42:D191–8.

Vedadi M, Lew J, Artz J, *et al*. (2007). Genome-scale protein expression and structural biology of *Plasmodium falciparum* and related Apicomplexan organisms. Mol Biochem Parasitol 151:100–10.

Wang J, Hartling JA, Flanagan JM. (1997). The structure of ClpP at 2.3 A resolution suggests a model for ATP-dependent proteolysis. Cell 91: 447–56.

Wang J, Hartling JA, Flanagan JM. (1998). Crystal structure determination of *Escherichia coli* ClpP starting from an EM-derived mask. J Struct Biol 124:151–63.

Ye F, Zhang J, Liu H, *et al*. (2013). Helix unfolding/refolding characterizes the functional dynamics of *Staphylococcus aureus* Clp protease. J Biol Chem 288:17643–53.

Zeiler E, List A, Alte F, *et al*. (2013). Structural and functional insights into caseinolytic proteases reveal an unprecedented regulation principle of their catalytic triad. Proc Natl Acad Sci USA 110:11302–7.

Zhang J, Ye F, Lan L, *et al*. (2011). Structural switching of *Staphylococcus aureus* Clp protease: a key to understanding protease dynamics. J Biol Chem 286:37590–601.